Molecular and Cellular Endocrinology 420 (2016) 159–168

Contents lists available at ScienceDirect

Molecular and Cellular Endocrinology

journal homepage: www.elsevier.com/locate/mce

Identification of a novel fusion transcript between human relaxin-1 (*RLN1*) and human relaxin-2 (*RLN2*) in prostate cancer

Gregor Tevz [a, 1], Sean McGrath [b], Ryan Demeter [b], Vincent Magrini [b], Varinder Jeet [a], Anja Rockstroh [a], Stephen McPherson [a], John Lai [a], Nenad Bartonicek [d], Jiyuan An [a], Jyotsna Batra [a], Marcel E. Dinger [d, e], Melanie L. Lehman [a, c], Elizabeth D. Williams [a], Colleen C. Nelson [a, c, *]

[a] Institute of Health and Biomedical Innovation, Australian Prostate Cancer Research Centre-Queensland, Queensland University of Technology/Translational Research Institute, Brisbane, QLD, Australia
[b] McDonnell Genome Institute, Washington University School of Medicine, St Louis, MO, USA
[c] Vancouver Prostate Centre, Department of Urologic Sciences, University of British Columbia, Vancouver, British Columbia, Canada
[d] Kinghorn Centre for Clinical Genomics, Garvan Institute of Medical Research, Sydney, Australia
[e] St Vincent's Clinical School, University of New South Wales, Sydney, Australia

ARTICLE INFO

Article history:
Received 10 August 2015
Received in revised form
13 October 2015
Accepted 16 October 2015
Available online 21 October 2015

Keywords:
Prostate cancer
RLN1
RLN2
Fusion
SMRT sequencing
RNA-Seq

ABSTRACT

Simultaneous expression of highly homologous *RLN1* and *RLN2* genes in prostate impairs their accurate delineation. We used PacBio SMRT sequencing and RNA-Seq in LNCaP cells in order to dissect the expression of *RLN1* and *RLN2* variants. We identified a novel fusion transcript comprising the *RLN1* and *RLN2* genes and found evidence of its expression in the normal and prostate cancer tissues. The *RLN1-RLN2* fusion putatively encodes RLN2 isoform with the deleted secretory signal peptide. The identification of the fusion transcript provided information to determine unique *RLN1-RLN2* fusion and *RLN1* regions. The *RLN1-RLN2* fusion was co-expressed with *RLN1* in LNCaP cells, but the two gene products were inversely regulated by androgens. We showed that *RLN1* is underrepresented in common PCa cell lines in comparison to normal and PCa tissue. The current study brings a highly relevant update to the relaxin field, and will encourage further studies of RLN1 and RLN2 in PCa and broader.

1. Introduction

Relaxin is a mammalian hormone that is involved in reproduction. As the name suggests, relaxin is the component of serum that causes the relaxation of the pubic ligament in pregnant female prior to delivery (Fevold et al., 1930; Hisaw, 1926). The human relaxin gene was first isolated from a cDNA library from the *corpus luteum*, and later confirmed and characterized by mass spectrometry (Hudson et al., 1984; Stults et al., 1990). In apes and humans, the relaxin gene underwent a duplication generating two relaxin genes with high sequence similarity, relaxin-1 (*RLN1*) and relaxin-2 (*RLN2*). (Arroyo et al., 2014; Crawford et al., 1984). *RLN1* mRNA is expressed in the prostate, but RLN1 peptide has never been isolated and its function has not been explored yet (Garibay-Tupas et al., 2000; Gunnersen et al., 1996). The ovaries and prostate are the two major sources of RLN2 in humans. The expression of RLN2 in ovaries is intermittent and increases during the luteal phase of the menstrual cycle, with highest levels being produced by the *corpus luteum* during pregnancy (Ivell et al., 1989). In men, RLN2 is produced continuously by the prostate, and accumulates in the seminal fluid to increase sperm motility (Carrell et al., 1995; Winslow et al., 1992). Outside normal physiology, RLN2 is a promoter of cancer progression in several different types of cancers (Nair et al.,

Abbreviations: CSS, CCS; *RLN1*, *RLN2*; *RLN1-RLN2*, *RLN1-RLN2-1*; *RLN1-RLN2-2*, PCa; SMRT, RNA-Seq; PacBio, SMRTBell; MISO, EST; FBS, DHT; R1881, BAM; shAR, shRLN2; shNT, RFP; dox, Hg19; Hg38, TCGA; TPM, *AR*; *PSA*, RNF6.

* Corresponding author. Australian Prostate Cancer Research Centre – Queensland, Institute of Health and Biomedical Innovation, Queensland University of Technology, Princess Alexandra Hospital, Translational Research Institute, Brisbane, Australia.
E-mail address: colleen.nelson@qut.edu.au (C.C. Nelson).
[1] Present address: Australian Prostate Cancer Research Centre-Queensland, Institute of Health and Biomedical Innovation, Queensland University of Technology, and Translational Research Institute, 37 Kent Street, Brisbane, Queensland 4102, Australia.

http://dx.doi.org/10.1016/j.mce.2015.10.011

2012). In prostate cancer (PCa), RLN2 was shown to promote tumor growth and vascularisation, and was regulated by androgens (Feng et al., 2010; Silvertown et al., 2006; Thompson et al., 2010, 2006). Inhibition of RLN2 signalling by a peptide antagonist in PCa showed promising therapeutic efficacy in preclinical studies (Feng et al., 2010; Neschadim et al., 2014).

High homology between RLN1 and RLN2 in the context of simultaneous expression in prostate tissue hinders the accurate characterization and functional study of individual relaxin genes in the prostate. In addition to the canonical sequences, a 101 bp longer alternatively spliced variant of *RLN2* was discovered in the prostate tissue (Gunnersen et al., 1996). There are several more transcript variants predicted by automated computational analysis that are supported by mRNA and EST data as annotated in the Aceview database (Thierry-Mieg and Thierry-Mieg, 2006). Standard mRNA determination methods like qPCR, microarray, and RNA-Seq all largely depend on gene annotation databases which are incomplete, and change frequently with the identification of novel transcripts. Recent development of PacBio single molecule real time (SMRT) sequencing techniques aids the identification of transcript variants due to the longer read lengths produced by this platform (Eid et al., 2009). Although PacBio data are inherently error-prone, a level of consensus accuracy can be achieved by multiple sequencing passes around the SMRTBell libraries. Circular consensus sequences (CCS) are derived from the long, raw reads providing sufficient read-of-insert depth of coverage to improve CCS read accuracy to >98% (Travers et al., 2010). Paired-end RNA-Seq can also be used to characterize the expression of alternatively spliced genes using a Sashimi Plot - this implements a mixture of isoforms (MISO) algorithm and displays alternative exon usage by splice junction reads as arcs connecting a pair of exons (Katz et al., 2015).

The aim of the present study was to use PacBio derived long cDNA SMRT sequencing in LNCaP cells in order to dissect the expression of *RLN1*, *RLN2*, and their transcript variants, and to identify unique *RLN1* and *RLN2* regions for the purpose of more accurate characterization. We report on a novel abundantly expressed fusion transcript between *RLN1* and *RLN2*. The *RLN1-RLN2* fusion putatively encodes an alternative RLN2 isoform with an altered signal sequence domain that potentially changes the mode of secretion. We inspected publically available RNA-Seq datasets for evidence of *RLN1-RLN2* fusion expression in normal and PCa tissues. The fusion has substantial sequence overlap with *RLN1* and *RLN2*, however we designed unique *RLN1-RLN2* fusion and *RLN1* qPCR primers, and determined their expression in common PCa cell lines as well as defined their androgen regulation.

2. Materials and methods

2.1. Cell lines

Immortalized prostate epithelial cells RWPE-1 (ATCC CRL-11609) were grown in keratinocyte serum-free media supplemented with recombinant human epidermal growth factor (5 ng/ml final concentration) and bovine pituitary extract (50 ng/ml). Immortalized prostate epithelial cells BPH-1, HPR-1, and PCa cell lines PC-3 (ATCC CRL-1435), 22RW1 (ATCC CRL-2505), DU145 (ATCC HTB-81), LNCaP (ATCC CRL-1740), C4-2B (from Dr Leland Chung, Cedars-Sinai Medical Center, USA), DuCaP (from Dr Matthias Nees, Faculty of Medicine, Turku University, Finland) were cultured in RPMI1640 supplemented with 5% FBS. LAPC4 cells were grown in IMDB medium supplemented with 5% FBS. HEK293T were cultured in high-glucose DMEM, supplemented with 2 mM L-glutamine and 1 mM sodium pyruvate and 10% heat inactivated FBS. All media and supplements were sourced from Gibco (Life Technologies, Mulgrave, VIC, AU). All cells were grown in a cell culture incubator at standard conditions (37 °C, 5% CO_2).

2.2. PacBio sequencing

Clontech SMARTer cDNA Synthesis. Long cDNA was prepared from 1 μg of DNase-treated LNCaP total RNA using the Clontech SMARter PCR Synthesis Kit (Clontech Laboratories, Mountain View, CA, USA). Second-strand cDNA was prepared in sixteen PCR reactions with 2 μl undiluted first-strand cDNA, 0.24 μM Clontech 5′ PCR Primer IIA and KAPA HiFi HotStart ReadyMix (Kapa Biosystems, Inc., Wilmington, MA, USA) for 14 cycles in the standard SMARTer PCR cycling conditions. The second-strand PCR production was purified and concentrated through a single QIAquick PCR Purification Kit (QIAGEN Sciences, Germantown, MD, USA) and the concentration was determined using the Qubit dsDNA HS Assay Kit (Life Technologies, Grand Island, NY, USA). *cDNA-Capture and Amplification*. The cDNA was hybridized with a custom NF1 probe set (Gutmann et al., 2013). Here, 780 ng of the cDNA library was mixed with 5 μg Cot-1 DNA (Invitrogen, Carlsbad, CA, USA) and 100 ng of NF1 probe. Hybridization was carried out in the presence of NimbleGen hybridization buffers (Roche NimbleGen, Madison, WI, USA) and processed per NimbleGen's SeqCap EZ Library SR user guide instructions. The solutions were denatured and allowed to hybridize at 47 °C for 72 h. Post hybridization and PCR steps are described in Cabanski et al. (2013). In brief, we performed 14 PCR cycles for the enriched cDNA library. *Pacific Biosciences Sample Prep and Sequencing*. Captured cDNA was converted into a 2 kb Pacific Biosciences (Pacific Biosciences of California, Inc., Menlo Park, CA, USA) library, according to the standard protocol using 500 ng of captured genomic DNA or cDNA and the DNA Template Prep Kit 2.0 (250 bp – 3 Kb). The resulting libraries were prepared for sequencing with the P4 polymerase and C2 chemistry using the MagBead protocol and DNA/Polymerase Binding Kit P4. The libraries complexes were prepared with 30 pM library and a 10:1 ratio of P4 DNA polymerase to library. Each library complex was sequenced on two SMRT cells with 180 min movie lengths using the MagBead Standard Seq v2 protocol. Circular consensus sequences were called using the ReadsOnInsert_CCS protocol through the SMRT Portal interface. The minimum full pass and minimum predicted accuracy filters were set at 2 and 90%, respectively. *Detection of RLN1-RLN2 fusion*. The *RLN1-RLN2* fusion was identified from full-length CCS reads spanning the length of the entire transcript. For a transcript to be reported, we required at least two independent CCS reads to contain identical nucleotide sequences over the entire length of the transcript.

2.3. Analysis of RNA-Seq

RNA-Seq from LNCaP cells. LNCaP cells were seeded in a 10 cm culture dish and treated with 10 nM dihydrotestosterone (DHT) as described in the section 'Short-term androgen deprivation assay' below. Total RNA was isolated using the Norgen RNA Plus extraction kit (Norgen, Acacia Ridge, QLD, AU). RNA-Seq was carried out on total RNA using an Illumina TruSeq Stranded mRNA Sample Prep Kit with Set A indexes (Illumina, Scoresby, VIC, AU) and sequenced on Illumina HiSeq2500 v4.0 platform (Kinghorn Centre for Clinical Genomics (KCCG), Sydney, NSW, AU). Sequencing reads were generated by quality trimming using Trimgalore v.03.7 (Babraham Institute, http://www.bioinformatics.babraham.ac.uk/projects/trim_galore/) and aligned to the GRCh38/hg38 genome using STAR v.2.4.0j (Dobin et al., 2013). *RNA-Seq from normal and PCa tissue*. Transcript splice-site usage was assessed on RNA-Seq data sets comprising 14 PCa tumors and adjacent benign tissue (Ren et al., 2012). RNA-Seq reads were mapped using Tophat2 (GRCh37/Hg19 assembly), and splice sites were visualized using

indexed BAM files and the Integrative Genomics Viewer (Kim et al., 2013; Robinson et al., 2011). IlluminaHiSeq_RNASeqV2 from 193 samples generated by the TCGA Research Network were accessed at http://cancergenome.nih.gov/(September 4, 2013) and were analysed as previously described (Li et al., 2010). *Correction of the RLN1-RLN2 fusion sequence informed by Illumina RNA-Seq from LNCaP cells*. We generated the bowtie (Langmead et al., 2009) index files for the corrected *RLN1-RLN2-2* fusion transcript sequence (genome assembly GRCh38/Hg38 matched). The reads from Illumina RNA-Seq from LNCaP cells were then aligned to the *RLN1-RLN2-2* fusion transcript and the bam file was generated and visualized in RNA-SeqBrower (An et al., 2015).

2.4. Inducible stable shRNA cell line models

Lentivirus particles were generated in HEK 293T host cells transfected with X-tremeGENE HP DNA Transfection Reagent (Roche, Sydney, NSW, AU) and inducible lentiviral pTRIPZ shRNA plasmids targeting either the androgen receptor (AR) (shAR), *RLN2* (shRLN2), or a negative control (shNT) (Thermo-Fisher Scientific, Richlands, QLD, AU). The pCMV-8.2R lentiviral packaging plasmids and pCMV-VSVG were kindly provided by Dr Brett Hollier (Queensland University of Technology, Brisbane, QLD, AU). Virus particles were collected 48 h and 72 h after transfection, and filtered through 45 μm filters. Target cells (LNCaP) were infected with the virus supernatant and 8 μg/ml protamine sulphate (Sigma–Aldrich, Castle Hill, NSW, AU). Transfected cells were then selected with 2 μg/ml Puromycin Dihydrochloride (Life Technologies, Mulgrave, VIC, Australia). We observed some cells expressing red fluorescent protein (RFP) indicating inducible promoter leakage; therefore we used an Astrios EQ cell sorter (Beckman Coulter, Lane Cove, QLD, Australia) to remove cells with leaky inducible promoter.

2.5. Inhibition of androgen signalling

Short-term androgen deprivation assay. LNCaP cells were seeded into T25 flasks, and incubated in RPMI1640 + 5% FBS for 3 days. The medium was then changed to RPMI 1640 supplemented with 5% charcoal stripped serum (CSS) and incubated for 2 days, then changed to RPMI 1640 supplemented with 10 nM DHT or 1 nM R1881, and incubated for 48 h with DHT top-up at 24 h. The reference group was kept in CSS. *Long-term androgen deprivation assay*. LNCaP cells were seeded into T25 flasks and incubated in RPMI 1640 + 5% FBS for 3 days. The medium was then changed to RPMI 1640 supplemented with 5% CSS, and incubated for 10 days with medium changes every 3 days. *Inducible AR knock-down*. LNCaP cells were seeded onto T25 flasks and incubated in RPMI 1640 + 5% FBS for 3 days. The medium was then changed to RPMI 1640 supplemented with 5% CSS, and incubated with or without 1 μg/ml of doxycyline (dox) for 48 h. The medium was then supplemented with 10 nM DHT, and incubated for 48 h. The reference group was kept in CSS.

2.6. Quantitative real-time PCR

Total RNA was extracted using the RNAeasy Kit (Qiagen, Chadstone Centre, VIC, AU) before reverse transcription with SuperScript III Reverse Transcriptase (Life Technologies, Mulgrave, VIC, AU) according to the manufacturer's protocol. Subsequent quantitative PCR (qPCR) was carried out on the ViiA7 or 7900HT Real-Time PCR System (Life Technologies, Mulgrave, VIC, AU) with SYBR Green, or using Universal TaqMan detection (Life Technologies, Mulgrave, VIC, AU). Gene expression was determined using the $2^{-\Delta\Delta Ct}$ method, and normalized to the housekeeping gene RPL32. Data is expressed relative to the reference group. Experiments were repeated a minimum of 3 times. Primer sequences are detailed in the Supplementary Table 1.

2.7. Statistical analysis

Results are representative of at least three independent experiments with triplicate samples generating similar findings. Differences between experimental groups were statistically evaluated by multiple t-tests, followed by the Holm–Sidak test for multiple comparisons. $p \leq 0.05$ was considered statistically significant. Statistical analysis was performed using Prism 6 (GraphPad Software Inc.).

3. Results

3.1. Identification of novel RLN1-RLN2 fusions in PCa

To comprehensively identify *RLN1* and *RLN2* transcript variants, we used long cDNA-Cap and SMRT sequencing in LNCaP cells, and queried for circular consensus sequences (CCSs) that mapped to the *RLN1-RLN2* locus. We found CCSs identical to the annotated *RLN1* gene, but interestingly, no CCS corresponded to the annotated *RLN2* gene (GENCODE Version 19). Instead, the search retrieved sequences of two longer *RLN2* transcript variants which were fused to the RLN1 gene, generating two fusion transcripts *RLN1-RLN2-1* and *RLN1-RLN2-2* (Fig. 1, Supplementary Fig. S1). The inherent error-proneness of the SMRT sequencing technology hindered the determination of the

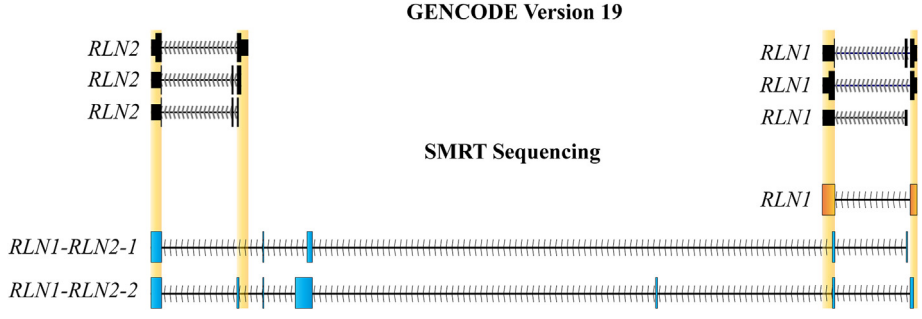

Fig. 1. Identification of the *RLN1-RLN2* fusion in LNCaP cells using SMRT sequencing. The figure was extracted from the UCSC Genome Browser where the circular consensus sequences (CCS) of *RLN1* and *RLN2* identified by SMRT sequencing were aligned to the *RLN1/RLN2* genomic locus using BLAT tool. GENCODE Version 19 annotated *RLN1* and *RLN2* transcript variants are shown in black. Combined CCS sequences of *RLN1* are shown in orange and *RLN1-RLN2* fusion CCS transcripts in blue. The arrowed-line represents introns and show directionality of the transcripts. The golden rectangles show an overlay between the annotated *RLN1* and *RLN2* and the transcripts identified by SMRT sequencing. (For interpretation of the references to color in this figure caption, the reader is referred to the web version of this article.)

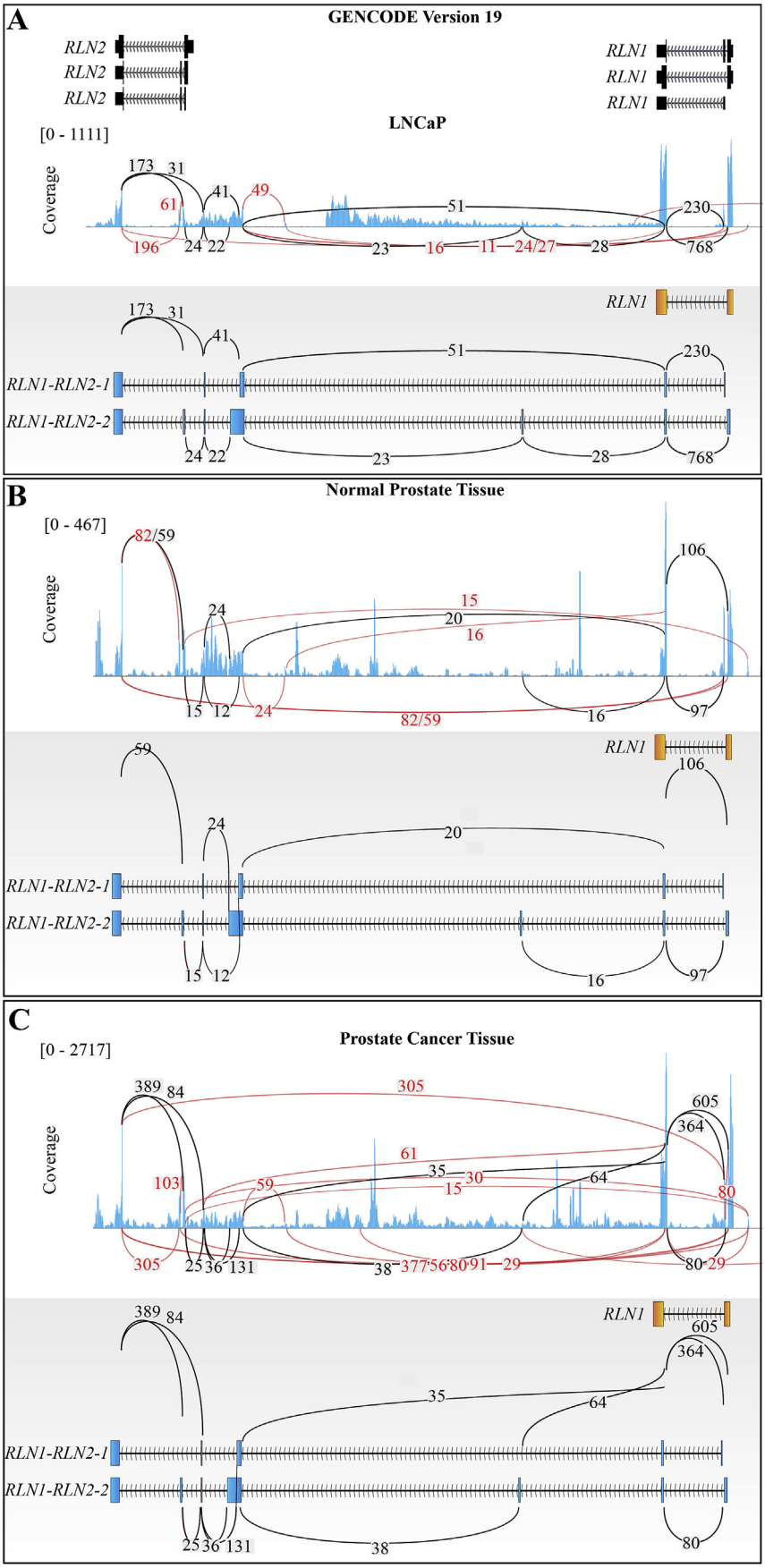
A
GENCODE Version 19
RLN2
RLN2
RLN2
RLN1
RLN1
RLN1
LNCaP
[0 - 1111]
Coverage
RLN1
RLN1-RLN2-1
RLN1-RLN2-2
B
Normal Prostate Tissue
[0 - 467]
Coverage
RLN1
RLN1-RLN2-1
RLN1-RLN2-2
C
Prostate Cancer Tissue
[0 - 2717]
Coverage
RLN1
RLN1-RLN2-1
RLN1-RLN2-2

precise nucleotide sequence of the fusion transcripts. Therefore, we aligned the sequences of the novel fusion transcripts *RLN1-RLN2-1* and *RLN1-RLN2-2* to the human genome assembly GRCh38/hg38 using the Blat tool in the UCSC genome browser (Kent, 2002; Kent et al., 2002). The sequences of the fusion transcripts were then corrected to match the genomic sequence. In order to increase the degree of certainty of the fusion transcript sequence, we mapped individual sequencing reads generated by a standard Illumina paired-end RNA-Seq from LNCaP cells to the corrected *RLN1-RLN2-2* fusion sequence. We utilized a recently in-house developed RNASeqBrowser tool (An et al., 2015) and observed that the raw sequencing reads perfectly aligned to the corrected sequence of the *RLN1-RLN2-2* fusion, confirming its legitimacy (Supplementary Fig. S2). The mapping of raw sequencing reads highlighted only 3 differences in the nucleotide sequence of the *RLN1-RLN2-2* fusion that could be ascribed to the difference between the human genome assembly GRCh38/hg38 and LNCaP genome (Supplementary Fig. S2). To additionally confirm the expression of the *RLN1-RLN2* fusion transcripts, we analysed Illumina paired-end RNA-Seq from LNCaP cells using Sashimi Plot representation of RNA-Seq data in the Integrative Genomic Viewer. Sashimi Plots display alternative exon usage by drawing splice junction reads as arcs connecting a pair of exons (Katz et al., 2015). Both novel fusion transcripts *RLN1-RLN2-1* and *RLN1-RLN2-2* were clearly observed in the Sashimi Plot of RNA-Seq from LNCaP cells (Fig. 2A). We then inspected Ren et al. RNA-Seq data comprising PCa tumors and adjacent benign tissue, and found similar splice junction reads between exons of novel fusion transcripts to those in LNCaP cells, suggesting broader representation of the *RLN1-RLN2* fusion (Fig. 2B, C) (Ren et al., 2012). In support of the newly identified RLN1-RLN2 fusion transcript the sequence of a similar longer *RLN2* variant was recently predicted by an automated computational analysis that was supported by mRNA and EST evidence (accession number: XM_011518003.1, March 2015) (Supplementary Fig. S3).

3.2. Novel RLN1-RLN2 fusion has an alternative putative ORF

The novel *RLN1-RLN2* fusion transcripts contained incomplete nucleotide sequences of both *RLN1* and *RLN2* and acquired novel exons in the intergenic region between the genes. In order to investigate whether the *RLN1-RLN2* fusion transcripts encode novel putative open reading frames (ORF) we analysed the sequences with the Translate Tool (Expasy, http://web.expasy.org/translate/). The shorter *RLN1-RLN2-1* fusion transcript putatively translated into a RLN2 peptide with a truncated C-peptide and an A-chain, and was therefore not considered for further investigation. The analysis of the longer *RLN1-RLN2-2* fusion transcript predicted a novel RLN2 isoform with an alternative start codon within a novel exon of the fusion (Fig. 3). The new putative RLN2 isoform contained intact functional domains of RLN2 (B-chain, C-peptide and A-chain), but lost the entire signal sequence that is essential for its secretion via the endoplasmic reticulum (ER)-Golgi secretory pathway (Fig. 3). Instead, the signal sequence was replaced by a short leader peptide MNTSKAVA (Fig. 3). We also unveiled an LNCaP specific single nucleotide polymorphism in the C-peptide region of *RLN2* (and of *RLN1-RLN2-2*) that affected the change of amino acid from isoleucine to asparagine in the sequence KKLI/NRNR (Supplementary Fig. S2).

3.3. Identification of unique RLN1-RLN2 fusion and RLN1 regions

The *RLN1-RLN2-2* fusion showed a significant overlap with the annotated *RLN1* and *RLN2* genes. In order to characterize the expression of the fusion, we aligned both novel fusion transcripts using the BLAT tool in the USCS genome browser (Kent, 2002; Kent et al., 2002), and designed the qPCR primers in unique *RLN1-RLN2-2* regions. The forward primer for specific detection of *RLN1-RLN2-2* fusion was designed to span the junction between the novel exon of the fusion and the downstream fusion exon that is shared with the annotated *RLN2*. The reverse primer was designed in a region shared by *RLN2* and *RLN1-RLN2-2* fusion (Fig. 4A). Similarly, we designed qPCR primers in the *RLN1* unique region (Fig. 4A). In order to test the specificity of the primers, we stably transfected LNCaP cells with a doxycycline inducible lentiviral vector encoding shRNA targeting the annotated *RLN2* gene (shRLN2). LNCaP cells stably expressing non-targeting shRNA (shNT) were used as a control. The addition of doxycycline in shNT cells had no effect on the expression of *RLN1-RLN2-2* fusion, whereas the addition of doxycycline to shRLN2 cells resulted in a significant decrease in the levels of *RLN1-RLN2-2* fusion (Fig. 4B). These results confirmed that the novel exon of the fusion is linked to the exon of the annotated *RLN2* gene. *RLN2* knock-down (shRLN2) had no effect on *RLN1* levels. Although the expression of *RLN1* decreased with doxycycline treatment, we observed no difference between the control (shNT) and shRLN2 cells, confirming the specificity of *RLN1* primers (Fig. 4C).

3.4. Underrepresentation of RLN1 in PCa cells

The *RLN1-RLN2-2* fusion and *RLN1* are overlapping same strand transcripts (Fig. 1). We thus predicted an association between the expression of *RLN1* and *RLN1-RLN2-2* fusion. We first determined the expression of *RLN1* in 3 normal and 7 PCa cell lines. *RLN1* was abundantly expressed only in LNCaP cells, whereas in other PCa cells, the expression was >80-fold lower (Fig. 5A). Similarly, the expression of the *RLN1-RLN2-2* fusion was highest in LNCaP cells, and marginal in the other PCa cells (Fig. 5B). The unexpected low expression of *RLN1* in common PCa cell lines was a surprising observation as *RLN1* is expressed in prostate tissue (Hansell et al., 1991). We found further evidence of prostate tissue specific expression of *RLN1* by accessing the Su et al. GeneAtlas microarray dataset (Fig. 5C) (Su et al., 2004). Next, we examined a publically available TCGA RNA-Seq dataset from normal and PCa tissue samples to investigate whether the expression of *RLN1* is limited to normal prostate tissue. We showed that both normal and PCa tissue expressed high levels of *RLN1* (Fig. 5D). The median expression of *RLN1* in normal prostate tissue was 42.5 transcripts per million reads (TPM) and 12.7 TPM in PCa tissue.

3.5. RLN1-RLN2 fusion and RLN1 are inversely regulated by androgens

The expression of *RLN2* has been shown to be negatively regulated by androgens in LNCaP cells (Thompson et al., 2006). The androgen responsiveness of *RLN2* led us to investigate the androgen

Fig. 2. *RLN1-RLN2* fusion exons were observed in RNA-Seq data from LNCaP and from normal and PCa tissues. Expression of transcripts at the *RLN1/RLN2* genomic locus is represented by a blue wiggle plot (RNA-Seq coverage). Arcs in the RNA-Seq coverage plot represent the junction between exons and the number informs the quantity of split reads between the exons. Black arcs show split reads between the exons of novel fusion transcripts *RLN1-RLN2-1* and *RLN1-RLN2-2* and the red arcs show the exon–exon junctions that were not identified by SMRT sequencing in LNCaP. The shadowed area shows an overlay of *RLN1* and novel *RLN1-RLN2* fusion transcripts with the junctions from RNA-Seq datasets generated using Sashimi Plot Tool and extracted from the Integrated Genome Viewer. A. GENCODE v.19 annotated *RLN1* and *RLN2* transcript variants (black) and RNA-Seq data from LNCaP cells. B. RNA-Seq data from Ren et al. (2012) study from benign prostate tissue and C. PCa tissue. (For interpretation of the references to color in this figure caption, the reader is referred to the web version of this article.)

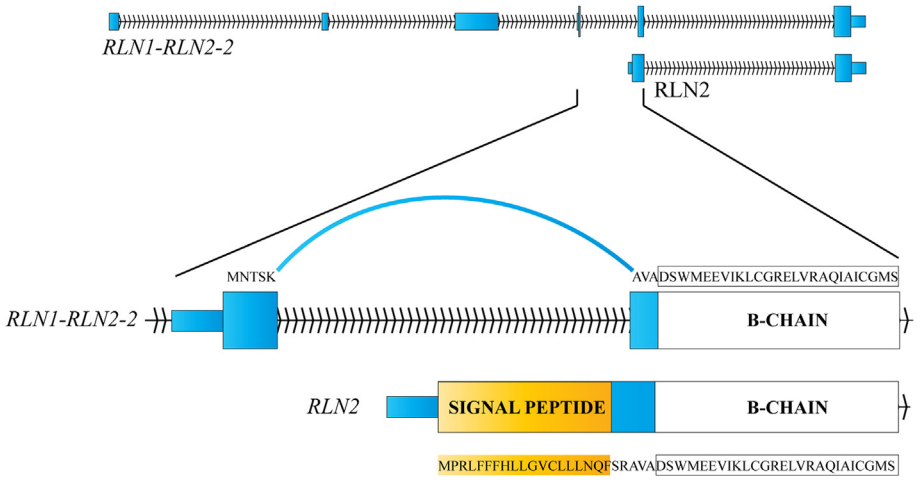

Fig. 3. *RLN1-RLN2-2* fusion encodes a putative RLN2 isoform without a signal peptide. Novel fusion *RLN1-RLN2-2* is aligned with the currently annotated RLN2 peptide. The region with an alternative start codon is enlarged below. The entire signal sequence is deleted in the novel putative RLN2 isoform however the functional B-chain, C-peptide and A-chain are unchanged (downstream C-peptide and A-chain not shown).

regulation of the *RLN1-RLN2-2* fusion and *RLN1*. Charcoal-stripped fetal bovine serum (CSS) was used to grow LNCaP cells in the absence of androgens for a period of 10 days. The removal of androgens resulted in a steady increase in the levels of the *RLN1-RLN2-2* fusion (Fig. 6A). Although the levels of *RLN1* were higher in the absence of androgens, the increase was marginal in comparison to the *RLN1-RLN2-2* fusion (Fig. 6A). To further confirm that the increase in expression of the *RLN1-RLN2-2* fusion was a result of androgens, we performed a similar experiment where LNCaP cells were first grown in CSS for 2 days followed by the 2 day treatment with androgens (10 nM DHT or 1 nM R1881). The treatment of LNCaP cells with androgens abolished the increase in expression of the *RLN1-RLN2-2* fusion (Fig. 6B). This androgen suppression resulted in 60–75% lower levels of *RLN1-RLN2-2* fusion in androgen treated cells compared to control (Fig. 6B). Contrary to the *RLN1-RLN2-2* fusion, the addition of androgens resulted in up-regulation of the expression of *RLN1*, indicating an inverse androgen regulation of the transcripts (Fig. 6C). To further assure that the inverse androgen regulation of *RLN1-RLN2-2* and *RLN1* is a result of androgen directed signalling, we specifically inhibited the AR by doxycycline induced shRNA knock-down (shAR). DHT treatment in control cells (shNT) suppressed the expression of *RLN1-RLN2-2* fusion in both doxycxyline induced and non-induced cells (Fig. 6D). This suppression was still evident in non-induced shAR cells, but doxycycline induced AR knock-down impaired this suppression, confirming that androgen signalling down-regulates

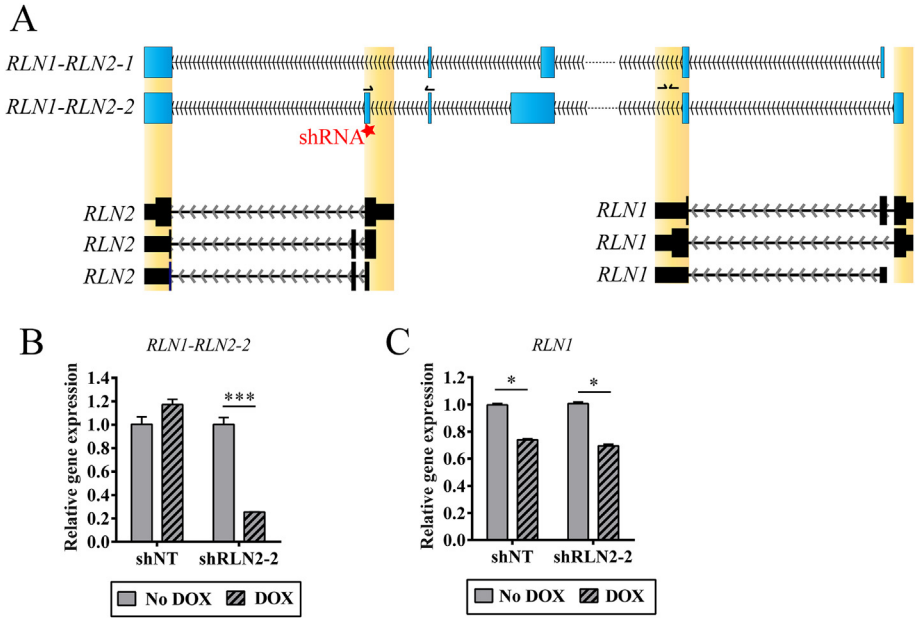

Fig. 4. Identification of unique sequences of *RLN1-RLN2-2* fusion and of *RLN1*. A. GENCODE V.19 *RLN1* and *RLN2* transcripts (black) are aligned to novel fusion transcripts *RLN1-RLN2-1* and *RLN1-RLN2-2*. The canonical exons of *RLN1* and *RLN2* are overlaid to the fusion transcripts (gold rectangle) demonstrating the shared and unique regions of the transcripts. The arrows above transcripts represent the position of unique primer sets and the star represent the shRNA target sequence. The expression of B. *RLN1-RLN2-2* and C. *RLN1* after the doxycycline (DOX, 250 ng/ml) inducible knock-down of *RLN2*. (n = 3; error bars, SE), *$p < 0.05$, ***$p < 0.005$. (For interpretation of the references to color in this figure caption, the reader is referred to the web version of this article.)

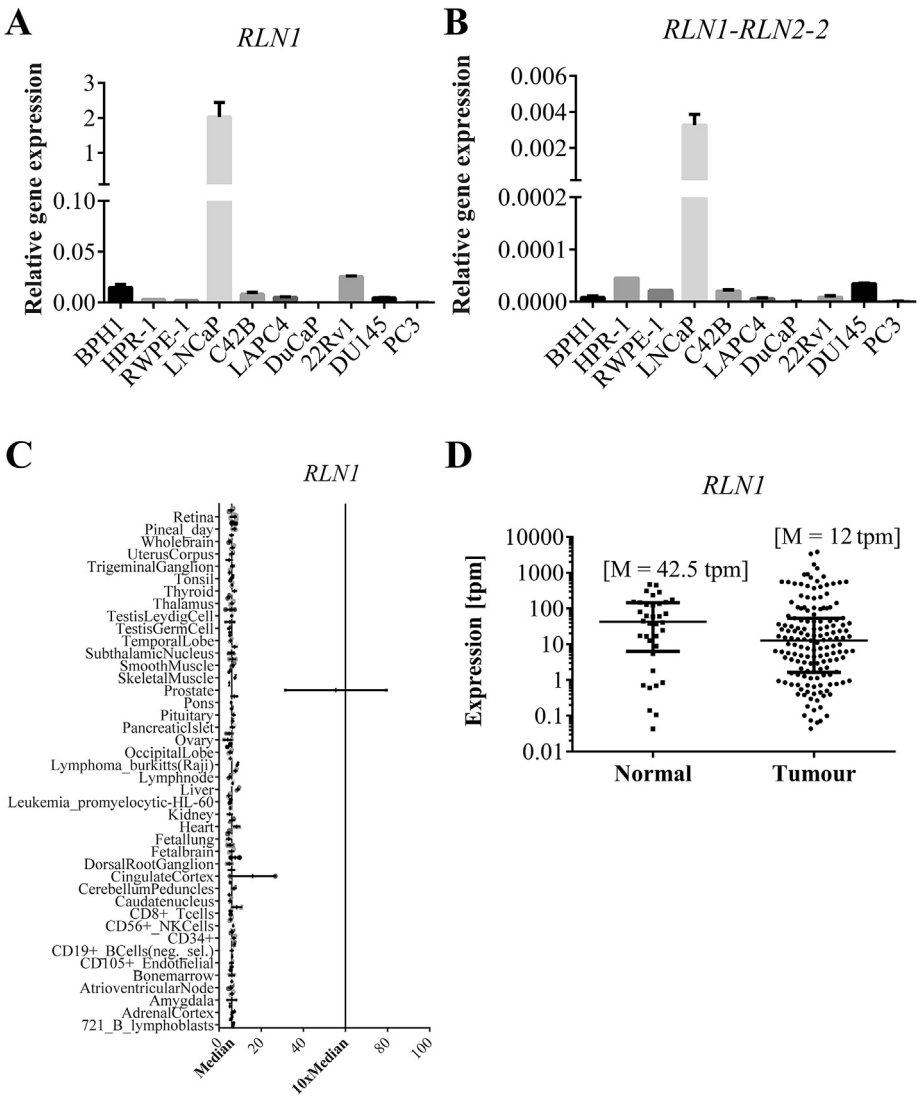

Fig. 5. Co-expression of *RLN1* and *RLN1-RLN2-2* fusion and underrepresentation of *RLN1* in PCa cell lines. Relative gene expression of A. *RLN1* and B. *RLN1-RLN2-2* in common PCa cell lines (n = 3; error bars, SE). C. The expression of *RLN1* in a publically available high-density microarray dataset from different human tissues (Su et al., 2004). The vertical line represents a 10× value of the Median expression in all tissues. The expression value for each tissue is an average of 2 microarray experiments with 11 probes for *RLN1*. D. Expression of *RLN1* determined from a TCGA RNA-Seq dataset from 36 benign prostate and 157 PCa tissues. The scatter plot represents expression values (transcripts per million, TPM) in each tissue sample; M (Median)

the levels of *RLN1-RLN2-2* (Fig. 6D). Contrary to *RLN1-RLN2-2*, the expression of *RLN1* was increased after DHT treatment in control cells, but this increase was suppressed by AR knock-down (Fig. 6E). The changes in expression of the androgen responsive gene PSA were determined in all assays to confirm that the levels of androgens were depleted, or that the AR knock-down was efficient, and AR signalling decreased (Supplementary Fig. S4).

4. Discussion

In this study we used SMRT sequencing of full length RNA transcripts in PCa LNCaP cells in order to dissect the expression of *RLN1*, *RLN2*, and their transcript variants, and to identify unique sequences of *RLN1* and *RLN2* for more accurate characterization. We report on a novel abundantly expressed fusion transcript comprising the *RLN1* and *RLN2* genes which encodes a putative RLN2 isoform with an altered signal sequence domain that potentially modifies its mode of secretion. By employing a Sashimi Plot visualization of RNA-Seq data, we showed the presence of the unannotated fusion in both normal and PCa tissue. We designed unique *RLN1-RLN2* fusion and *RLN1* qPCR primers, and found that the *RLN1-RLN2* fusion and *RLN1* were co-expressed in various PCa cell lines but inversely regulated by androgens in LNCaP cells. We showed that *RLN1* was surprisingly underrepresented in PCa cell lines in comparison to normal and PCa tissue.

We have identified a novel longer *RLN2* transcript variant representing a fusion between *RLN1* and *RLN2* in LNCaP cells (Fig. 1). Despite the use of northern blotting in previous PCa studies, longer *RLN2* transcripts have not been observed (Ivell et al., 1989). We have however used a recent state of the art SMRT sequencing technique and obtained *RLN1-RLN2* fusion sequences in PCa cells (Fig. 1). Additionally, we have observed fusion specific exons in RNA-Seq from normal and PCa tissues (Fig. 2B, C). Further evidence of the *RLN1-RLN2* fusion comes from a recent study where several longer RLN2 transcripts were predicted from de novo assembly of 7256 RNA sequencing (RNA-seq) libraries of tumors, normal tissue, and cell lines from 25 independent studies (Supplementary Fig. S5) (Iyer et al., 2015). The size of the fusion transcript was 2 kbp,

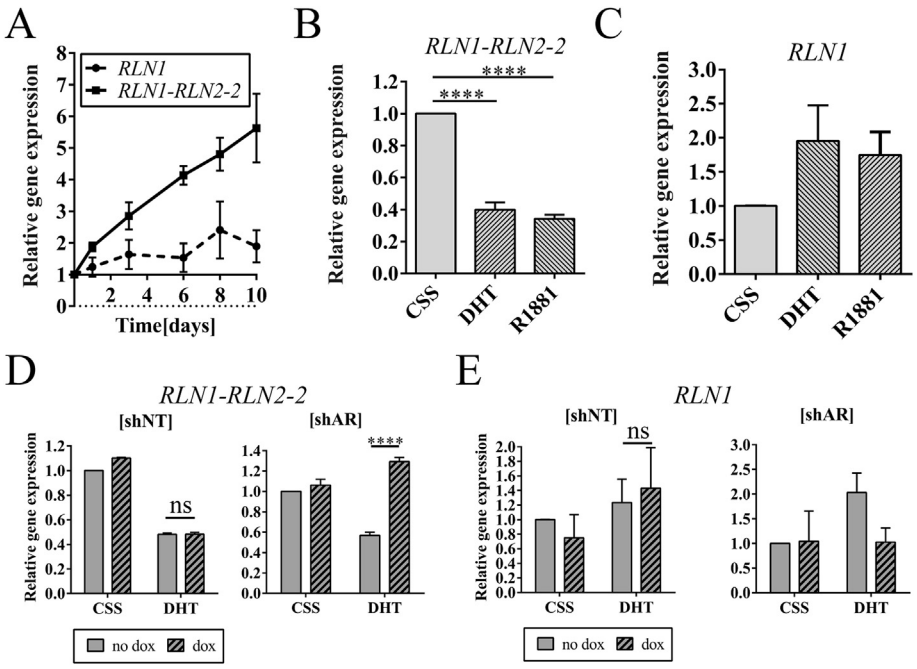

Fig. 6. *RLN1-RLN2-2* and *RLN1* are inversely regulated by androgens. A. Relative gene expression of *RLN1-RLN2-2* and *RLN1* determined in a long-term androgen deprivation assay; *RLN1-RLN2-2* (square), *RLN1* (circle). B. Relative gene expression of *RLN1-RLN2-2* and C. *RLN1* determined in a short-term androgen deprivation assay; CSS (absence of androgens), DHT (physiological androgen, 10 nM), R1881 (synthetic androgen, 1nM), (n = 3, error bars, SE). ****p < 0.001. D. Relative gene expression of *RLN1-RLN2-2* and E. *RLN1* in LNCaP cells stably expressing doxycycline (dox) inducible non-targeting shRNA [shNT] or shRNA targeting AR [shAR] determined in a short-term androgen deprivation assay; CSS (absence of androgens), DHT (physiological androgen, 10 nM), (n = 3, error bars, SE). ****p<0.001; ns -non significant.

making it twice the size of either *RLN1* or *RLN2*. The expression and tissue specificity of *RLN1*, *RLN2*, and their variants, has been previously investigated using cloning techniques from cDNA libraries, northern blotting and qPCR (Garibay-Tupas et al., 2000; Gunnersen et al., 1996; Hudson et al., 1984). Interestingly, initial northern blots performed in RNA samples from ovaries with *RLN2* specific probes revealed a longer transcript of the similar size (2 kbp) as the fusion transcript we identified in PCa cells LNCaP (Hudson et al., 1984). The longer variant was considered to be a potentially longer primary *RLN2* mRNA species that was probably truncated into a mature *RLN2* by cleavage in the alternative polyadenylation site but this had not been explored further. In another study, the longer 2 kbp variant of *RLN2* was confirmed by northern blotting in ovaries, and interestingly the expression was found to be increasing with the luteal phase of the menstrual cycle (Ivell et al., 1989). Thus, the evidence from the literature indicates that the longer *RLN2* transcripts observed in the ovarian samples resemble the size of the novel *RLN1-RLN2* fusion transcript identified in our study. Therefore, it would be interesting to investigate the expression of the *RLN1-RLN2* fusion in ovaries.

The novel *RLN1-RLN2* fusion putatively encodes a RLN2 isoform that retains all the functional domains of RLN2, but lacking the signal sequence responsible for secretion through the ER-Golgi complex and release into the cell exterior. The lack of a secretory signal could therefore obstruct the secretion of the RLN2 peptide from the cells. However, some secretory proteins lack the signal peptide and utilize alternative secretory pathways. For example, IL1β is a secretory inflammatory cytokine without a signal sequence and was consequently not found in the ER or Golgi but instead was translated by free polyribosomes (Lopez-Castejon and Brough, 2011). One of the proposed secretory pathways of IL1β included shedding by microvesicles or exosomes. Interestingly, prostate gland epithelial cells are known to secrete vesicles called prostasomes into the seminal fluid (Sahlen et al., 2002). Thus, it is possible that the fusion encoded RLN2 isoform is secreted from prostate cells enclosed in prostasomes. The membrane enclosed RLN2 would have limited functionality in the seminal fluid and would be protected from degradation until reaching the target tissue. Opposing to the hypothesis of the prostasomal secretion of the fusion encoded RLN2, the RLN2 peptide identified in the seminal fluid was identical to the one isolated from the ovaries thus without a fusion specific alternative MNTSKAVA leader sequence (Winslow et al., 1992). However in the mentioned study, RLN2 peptide was enriched from the sample of seminal fluid with an RLN2 antibody that might have failed to recognize the fusion encoded RLN2. In order to further investigate the cellular trafficking and function of the novel fusion encoded RLN2 isoform we aim to determine the precise nucleotide sequence of the fusion by sequencing of the cDNA clones and investigating its role in the next phase of our study.

The *RLN1-RLN2* fusion has a significant overlap with *RLN1* and *RLN2* and thus unique regions are severely restricted (Figs. 1 and 3), providing technical challenges for the accurate characterization of their expression. The fusion transcript overlapped the 3′ end of the first and the 5′ end of the second *RLN1* exon, which represents a prime template for qPCR primers to be able to discriminate between mRNA and genomic DNA. However in the case of *RLN1*, primers designed near the exon junction would not be able to discriminate between *RLN1* and *RLN1-RLN2* fusion transcripts. Therefore we designed qPCR primers in unique *RLN1* regions at the 3′ end of the second exon. *RLN1* specific primers were used previously, however their specificity was determined based on testing of different primer sets and selecting for those that were able to discriminate between the expression of *RLN1* in *corpus luteum* and prostate tissue. For instance, *RLN1* has been shown to be expressed in prostate tissue but not in the *corpus luteum* by northern blotting (Garibay-Tupas et al., 2000; Gunnersen et al., 1996). Confirming the validity of our unique *RLN1* region, the reverse primer for *RLN1* in

both studies was designed in a region that we identified to be unique for *RLN1* (Fig. 4).

Using our specific *RLN1* qPCR primers, we observed that *RLN1* mRNA is underrepresented in PCa cell lines. We found that *RLN1* was abundantly expressed only in LNCaP cells out of the 3 normal and 7 PCa cell lines tested. However, *RLN1* has been shown to be expressed in the prostate tissue (Gunnersen et al., 1996; Hansell et al., 1991). Specifically, we showed that RLN1 is a unique prostate tissue transcript (Fig. 5C) and abundantly expressed in normal prostate and cancer tissue (Fig. 5D). Thus, LNCaP cells best reflect the *RLN1* expression observed in PCa and is the most relevant cell line for the use in further studies of RLN1 biology.

Androgens and androgen-regulated genes are important in the onset and progression of PCa. We observed that the *RLN1-RLN2* fusion is down-regulated by androgens (Fig. 6B). The suppression of annotated *RLN2* was previously shown in LNCaP cells and tissues, however the primers used were unable to distinguish between *RLN2* and the *RLN1-RLN2* fusion (Thompson et al., 2006). In the later study, the *RLN1-RLN2* fusion transcript might have contributed to the majority of the qPCR signal considering the abundant expression of the fusion in LNCaP cells. Androgen regulation of *RLN1* has not been previously shown, although Xu et al. showed AR binding upstream of the *RLN1* gene, and co-regulation of *RLN1* expression by AR and RNF6 (Xu et al., 2009). We demonstrate that *RLN1* was up-regulated by androgens (Fig. 6C, E). Thus, we show here that although both *RLN1* and the *RLN1-RLN2* fusion transcript initiate from the same genomic locus and share parts of the genomic code, they are nevertheless inversely regulated by androgens. Since the transcription start site of *RLN1* is located just upstream of the *RLN1-RLN2* fusion, it would be interesting to investigate to what extent the transcription of *RLN1* directly controls the expression of the fusion transcript.

In conclusion, our study implemented a state of the art SMRT sequencing technique in LNCaP cells, and identified a novel fusion transcript comprising the *RLN1* and *RLN2* genes. The fusion transcript encodes a putative RLN2 with a deleted secretory signal peptide indicating a potentially biologically important alteration. We have unveiled an association between the expression and regulation of *RLN1-RLN2* fusion and *RLN1*, and discovered a surprising underrepresentation of *RLN1* in PCa cell lines. Although *RLN1-RLN2* was identified in PCa cells, we show evidence of its expression in normal prostate tissue. Further characterization of the *RLN1-RLN2* fusion product will shed new light on its role in PCa as well as foster fundamental research in the field.

Acknowledgements

This work was supported by the Australian Government Department of Health; the Movember Foundation and the Prostate Cancer Foundation of Australia through a Movember Revolutionary Team Award.

Appendix A. Supplementary data

Supplementary data related to this article can be found at http://dx.doi.org/10.1016/j.mce.2015.10.011.

References

An, J., Lai, J., Wood, D.L., Sajjanhar, A., Wang, C., Tevz, G., Lehman, M.L., Nelson, C.C., 2015. RNASeqBrowser: a genome browser for simultaneous visualization of raw strand specific RNAseq reads and UCSC genome browser custom tracks. BMC Genom. 16, 145.

Arroyo, J.I., Hoffmann, F.G., Opazo, J.C., 2014. Evolution of the relaxin/insulin-like gene family in anthropoid primates. Genome Biol. Evol. 6, 491–499.

Cabanski, C.R., Wilkerson, M.D., Soloway, M., Parker, J.S., Liu, J., Prins, J.F., Marron, J.S., Perou, C.M., Hayes, D.N., 2013. BlackOPs: increasing confidence in variant detection through mappability filtering. Nucleic Acids Res. 41, e178.

Carrell, D.T., Peterson, C.M., Urry, R.L., 1995. The binding of recombinant human relaxin to human spermatozoa. Endocr. Res. 21, 697–707.

Crawford, R.J., Hudson, P., Shine, J., Niall, H.D., Eddy, R.L., Shows, T.B., 1984. Two human relaxin genes are on chromosome 9. Embo J. 3, 2341–2345.

Dobin, A., Davis, C.A., Schlesinger, F., Drenkow, J., Zaleski, C., Jha, S., Batut, P., Chaisson, M., Gingeras, T.R., 2013. STAR: ultrafast universal RNA-seq aligner. Bioinformatics 29, 15–21.

Eid, J., Fehr, A., Gray, J., Luong, K., Lyle, J., Otto, G., Peluso, P., Rank, D., Baybayan, P., Bettman, B., Bibillo, A., Bjornson, K., Chaudhuri, B., Christians, F., Cicero, R., Clark, S., Dalal, R., Dewinter, A., Dixon, J., Foquet, M., Gaertner, A., Hardenbol, P., Heiner, C., Hester, K., Holden, D., Kearns, G., Kong, X., Kuse, R., Lacroix, Y., Lin, S., Lundquist, P., Ma, C., Marks, P., Maxham, M., Murphy, D., Park, I., Pham, T., Phillips, M., Roy, J., Sebra, R., Shen, G., Sorenson, J., Tomaney, A., Travers, K., Trulson, M., Vieceli, J., Wegener, J., Wu, D., Yang, A., Zaccarin, D., Zhao, P., Zhong, F., Korlach, J., Turner, S., 2009. Real-time DNA sequencing from single polymerase molecules. Science 323, 133–138.

Feng, S., Agoulnik, I.U., Truong, A., Li, Z., Creighton, C.J., Kaftanovskaya, E.M., Pereira, R., Han, H.D., Lopez-Berestein, G., Klonisch, T., Ittmann, M.M., Sood, A.K., Agoulnik, A.I., 2010. Suppression of relaxin receptor RXFP1 decreases prostate cancer growth and metastasis. Endocr-Relat Cancer 17, 1021–1033.

Fevold, H.L., Hisaw, F.L., Meyer, R.K., 1930. The relaxative hormone of the corpus luteum. Its purification and concentration. J. Am. Chem. Soc. 52, 3340–3348.

Garibay-Tupas, J.L., Bao, S., Kim, M.T., Tashima, L.S., Bryant-Greenwood, G.D., 2000. Isolation and analysis of the 3′-untranslated regions of the human relaxin H1 and H2 genes. J. Mol. Endocrinol. 24, 241–252.

Gunnersen, J.M., Fu, P., Roche, P.J., Tregear, G.W., 1996. Expression of human relaxin genes: characterization of a novel alternatively-spliced human relaxin mRNA species. Mol. Cell. Endocrinol. 118, 85–94.

Gutmann, D.H., McLellan, M.D., Hussain, I., Wallis, J.W., Fulton, L.L., Fulton, R.S., Magrini, V., Demeter, R., Wylie, T., Kandoth, C., Leonard, J.R., Guha, A., Miller, C.A., Ding, L., Mardis, E.R., 2013. Somatic neurofibromatosis type 1 (NF1) inactivation characterizes NF1-associated pilocytic astrocytoma. Genome Res. 23, 431–439.

Hansell, D.J., Bryant-Greenwood, G.D., Greenwood, F.C., 1991. Expression of the human relaxin H1 gene in the decidua, trophoblast, and prostate. J. Clin. Endocrinol. Metab. 72, 899–904.

Hisaw, F.L., 1926. Experimental relaxation of the pubic ligament of the guinea pig. P Soc. Exp. Biol. Med. 23, 661–663.

Hudson, P., John, M., Crawford, R., Haralambidis, J., Scanlon, D., Gorman, J., Tregear, G., Shine, J., Niall, H., 1984. Relaxin gene expression in human ovaries and the predicted structure of a human preprorelaxin by analysis of cDNA clones. Embo J. 3, 2333–2339.

Ivell, R., Hunt, N., Khan-Dawood, F., Dawood, M.Y., 1989. Expression of the human relaxin gene in the corpus luteum of the menstrual cycle and in the prostate. Mol. Cell. Endocrinol. 66, 251–255.

Iyer, M.K., Niknafs, Y.S., Malik, R., Singhal, U., Sahu, A., Hosono, Y., Barrette, T.R., Prensner, J.R., Evans, J.R., Zhao, S., Poliakov, A., Cao, X., Dhanasekaran, S.M., Wu, Y.M., Robinson, D.R., Beer, D.G., Feng, F.Y., Iyer, H.K., Chinnaiyan, A.M., 2015. The landscape of long noncoding RNAs in the human transcriptome. Nat. Genet. 47, 199–208.

Katz, Y., Wang, E.T., Silterra, J., Schwartz, S., Wong, B., Thorvaldsdottir, H., Robinson, J.T., Mesirov, J.P., Airoldi, E.M., Burge, C.B., 2015. Quantitative visualization of alternative exon expression from RNA-seq data. Bioinformatics 31, 2400–2402.

Kent, W.J., 2002. BLAT – the BLAST-like alignment tool. Genome Res. 12, 656–664.

Kent, W.J., Sugnet, C.W., Furey, T.S., Roskin, K.M., Pringle, T.H., Zahler, A.M., Haussler, D., 2002. The human genome browser at UCSC. Genome Res. 12, 996–1006.

Kim, D., Pertea, G., Trapnell, C., Pimentel, H., Kelley, R., Salzberg, S.L., 2013. TopHat2: accurate alignment of transcriptomes in the presence of insertions, deletions and gene fusions. Genome Biol. 14, R36.

Langmead, B., Trapnell, C., Pop, M., Salzberg, S.L., 2009. Ultrafast and memory-efficient alignment of short DNA sequences to the human genome. Genome Biol. 10, R25.

Li, B., Ruotti, V., Stewart, R.M., Thomson, J.A., Dewey, C.N., 2010. RNA-Seq gene expression estimation with read mapping uncertainty. Bioinformatics 26, 493–500.

Lopez-Castejon, G., Brough, D., 2011. Understanding the mechanism of IL-1beta secretion. Cytokine Growth Factor Rev. 22, 189–195.

Nair, V.B., Samuel, C.S., Separovic, F., Hossain, M.A., Wade, J.D., 2012. Human relaxin-2: historical perspectives and role in cancer biology. Amino Acids 43, 1131–1140.

Neschadim, A., Pritzker, L.B., Pritzker, K.P.H., Branch, D.R., Summerlee, A.J.S., Trachtenberg, J., Silvertown, J.D., 2014. Relaxin receptor antagonist AT-001 synergizes with docetaxel in androgen-independent prostate xenografts. Endocr-Relat Cancer 21, 458–471.

Ren, S., Peng, Z., Mao, J.H., Yu, Y., Yin, C., Gao, X., Cui, Z., Zhang, J., Yi, K., Xu, W., Chen, C., Wang, F., Guo, X., Lu, J., Yang, J., Wei, M., Tian, Z., Guan, Y., Tang, L., Xu, C., Wang, L., Gao, X., Tian, W., Wang, J., Yang, H., Wang, J., Sun, Y., 2012. RNA-seq analysis of prostate cancer in the Chinese population identifies recurrent gene fusions, cancer-associated long noncoding RNAs and aberrant alternative splicings. Cell Res. 22, 806–821.

Robinson, J.T., Thorvaldsdottir, H., Winckler, W., Guttman, M., Lander, E.S., Getz, G.,

Mesirov, J.P., 2011. Integrative genomics viewer. Nat. Biotechnol. 29, 24–26.
Sahlen, G.E., Egevad, L., Ahlander, A., Norlen, B.J., Ronquist, G., Nilsson, B.O., 2002. Ultrastructure of the secretion of prostasomes from benign and malignant epithelial cells in the prostate. Prostate 53, 192–199.
Silvertown, J.D., Ng, J., Sato, T., Summerlee, A.J., Medin, J.A., 2006. H2 relaxin overexpression increases in vivo prostate xenograft tumor growth and angiogenesis. Int. J. Cancer 118, 62–73.
Stults, J.T., Bourell, J.H., Canovadavis, E., Ling, V.T., Laramee, G.R., Winslow, J.W., Griffin, P.R., Rinderknecht, E., Vandlen, R.L., 1990. Structural characterization by mass-spectrometry of native and recombinant human relaxin. Biomed. Environ. Mass 19, 655–664.
Su, A.I., Wiltshire, T., Batalov, S., Lapp, H., Ching, K.A., Block, D., Zhang, J., Soden, R., Hayakawa, M., Kreiman, G., Cooke, M.P., Walker, J.R., Hogenesch, J.B., 2004. A gene atlas of the mouse and human protein-encoding transcriptomes. P Natl. Acad. Sci. U. S. A. 101, 6062–6067.
Thierry-Mieg, D., Thierry-Mieg, J., 2006. AceView: a comprehensive cDNA-supported gene and transcripts annotation. Genome Biol. 7.
Thompson, V.C., Hurtado-Coll, A., Turbin, D., Fazli, L., Lehman, M.L., Gleave, M.E., Nelson, C.C., 2010. Relaxin drives Wnt signaling through upregulation of PCDHY in prostate cancer. Prostate 70, 1134–1145.
Thompson, V.C., Morris, T.G.W., Cochrane, D.R., Cavanagh, J., Wafa, L.A., Hamilton, T., Wang, S.Y., Fazli, L., Gleave, M.E., Nelson, C.C., 2006. Relaxin becomes upregulated during prostate cancer progression to androgen independence and is negatively regulated by androgens. Prostate 66, 1698–1709.
Travers, K.J., Chin, C.S., Rank, D.R., Eid, J.S., Turner, S.W., 2010. A flexible and efficient template format for circular consensus sequencing and SNP detection. Nucleic Acids Res. 38, e159.
Winslow, J.W., Shih, A., Bourell, J.H., Weiss, G., Reed, B., Stults, J.T., Goldsmith, L.T., 1992. Human seminal relaxin is a product of the same gene as human luteal relaxin. Endocrinology 130, 2660–2668.
Xu, K., Shimelis, H., Linn, D.E., Jiang, R., Yang, X., Sun, F., Guo, Z., Chen, H., Li, W., Chen, H., Kong, X., Melamed, J., Fang, S., Xiao, Z., Veenstra, T.D., Qiu, Y., 2009. Regulation of androgen receptor transcriptional activity and specificity by RNF6-induced ubiquitination. Cancer Cell 15, 270–282.